Continuous-Variable QKD with key rates far above Devetak-Winter

Arpan Akash Ray[1] and Boris Škorić[1]

[1] *TU Eindhoven, The Netherlands*

Abstract

Continuous-Variable Quantum Key Distribution (CVQKD) at large distances has such high noise levels that the employed error-correcting codes must have very low rate. In this regime it becomes feasible to implement random-codebook error correction, which is known to perform close to capacity.

We propose a random-codebook reverse reconciliation scheme for CVQKD that is inspired by spread-spectrum watermarking. Our scheme has a novel way of achieving statistical decoupling between the publicly sent reconciliation data and the secret key. We provide a theoretical analysis of the secret key rate and we present numerical results. The best performance is obtained when the message size exceeds the mutual information $I(X;Y)$ between Alice and Bob's measurements. This somewhat counter-intuitive result is understood from a tradeoff between code rate and frame rejection rate, combined with the fact that error correction for QKD needs to reconcile only random data. We obtain secret key lengths that lie far above the Devetak-Winter value $I(X;Y) - I(E;Y)$.

1 Introduction

1.1 Error correction in Continuous-Variable QKD

Continuous-Variable Quantum Key Distribution (CVQKD) is a variant of QKD that works with weak coherent states and quadrature measurements. It is an attractive QKD variant because of its cost-effectiveness, which is due to the use of standard telecom equipment.

In Discrete-Variable QKD (DVQKD), propagation of light over long distances causes photon loss, which leads to non-detection events at the receiver side. The loss is very easy to deal with: the event is simply discarded. In CVQKD, in contrast, a quadrature observation always results in a measurement outcome. The loss of photons causes a deterioration of the signal-to-noise ratio (SNR) at the receiver's side. The extremely low SNR has to be dealt with by using high-performance error correcting codes. Various codes have been considered for CVQKD. Popular types of code are LDPC codes [1, 2, 3, 4, 5], Turbo codes and Polar codes [6, 7], all of which approach the Shannon limit. (See [8] for an overview.) In QKD it is important not only to be able to correct the errors, but also to do it *in real time*. This is a particularly tough challenge for the decoding step, which is the most computationally demanding. LDPC decoding, for instance, at low rate needs many iterations which cannot be done in parallel.

1.2 Contribution

We propose a reverse reconciliation scheme for long-distance CVQKD. Our scheme is essentially random codebook error correction. The codewords are random sequences. Bob performs a modular addition on his measurement sequence Y and a randomly chosen codeword, and sends the result to Alice, who then tries to reconstruct the codeword from this data and her own sequence X. Alice does a binary Neyman-Pearson test for each candidate codeword from the codebook. She *rejects* unless there is exactly one candidate on the right side of the decsion threshold. The use of random codebooks is motivated by two observations: (i) random codebooks get close to the Shannon limit;

(ii) at the very low rates dictated by long-distance CVQKD, the number of codewords in a code is limited and it becomes feasible to actually implement a random codebook.
In information reconciliation it is advantageous to work with 'decoupled' error correction data, i.e. data that is statistically independent from the secret that Alice and Bob establish. We achieve decoupling by first mapping Bob's measurements, which are Gaussian-distributed, to uniform variables on the interval $(0, 1)$ and then adding these values (modulo 1) to the random codeword entries which are also uniform on $(0, 1)$. In Discrete Variable QKD the equivalent would be to XOR a binary codeword into a binarisation of Y. Our decoupling technique is more versatile than the octonion-based approach of Leverrier et al [9], and avoids their 'no go theorem' that allows only 8-dimensional subspaces. Furthermore, our processing of Y retains distance information that is lost in common techniques like bit slicing [10] and Gray coding.
We present a theoretical analysis of our scheme as well as numerical results, working with Gaussian modulation for simplicity and ignoring detector inefficiency and electronic noise. We focus on small values of the transmission parameter. Having the option of accepting/rejecting yields an expression for secret key rate of the form

$$P_{\text{acc}}\Big[\gamma \cdot \big(1 - h(\text{BER})\big) \cdot I(X_i; Y_i) - I(E_i; Y_i)\Big]. \tag{1}$$

Here P_{acc} is the accept probability, X_i is Alice's i'th quadrature value, Y_i is Bob's corresponding quadrature, E_i is Eve's quantum system, I stands for mutual information, h is the binary entropy function, BER is the bit error rate in the accepted blocks, and γ represents the rate of our error-correcting code relative to the channel capacity $I(X_i; Y_i)$. It turns out that the highest key rate is obtained by setting $\gamma > 1$, even though this causes a high frame reject rate (low P_{acc}). Setting $\gamma > 1$ is allowed because in QKD Bob does not need to send a predetermined message to Alice; Bob and Alice only have to agree on a joint noise-free random string, which they can achieve even when the frame reject rate is close to 100%. (Using a code for CVQKD at a rate above capacity is a known option [11].)
Notably, the key rate obtained in this way can lie above the Devetak-Winter value $I(X_i; Y_i) - I(E_i; Y_i)$ which is often treated as a de facto upper bound on the secret key rate. The difference grows large if Alice can increase the laser power without causing problematic noise levels on Bob's side. Though surprising, the above-Devetak-Winter result is not mysterious. The security proof which shows that CVQKD key length $I(X; Y) - I(E; Y)$ is safe to use also predicts, when adapted to the existence of an accept/reject mechanism, that (1) is a safe to use key rate for any choice of γ.
Implementations of our scheme are necessarily brute-force, with limited opportunity for tricks to improve the computational load of decoding. Fortunately, the computation of Neyman-Pearson scores lends itself to massively parallel computation; hence we are cautiously optimistic about the feasibility of realtime implementation.
The outline of the paper is as follows. Section 2 contains preliminaries. In Section 3 we give the details of the proposed scheme. In Section 4 we analyse the scheme, computing statistical properties of the Neyman-Pearson scores and determining the key rate. Numerical results are presented in Section 5. In Section 6 we discuss implementation options, and Section 7 ends with concluding remarks.

2 Preliminaries

2.1 Notation and terminology

Stochastic variables are written in capital letters, and their numerical values in lowercase. The notation $\Pr[X = x]$ stands for the probability that the random variable X takes value x. The expectation over X is defined as $\mathbb{E}_x f(x) = \sum_x \Pr[X = x] f(x)$. The Shannon entropy of a random variable X is denoted as $\mathsf{H}(X)$. We write h for the binary entropy function, $h(p) = p \log \frac{1}{p} + (1 - p) \log \frac{1}{1-p}$. The notation 'log' is always base 2, and 'ln' is the natural logarithm. We measure all entropies in bits. The mutual information between X and Y is written as $I(X; Y)$. The entropy of Y given X is written as $\mathsf{H}(Y|X) = \mathbb{E}_x \mathsf{H}(Y|X = x)$.

A quantum state is described by a density matrix ρ. We write $S(\rho)$ for the von Neumann entropy of ρ. Consider a joint classical-quantum state of a classical random variable Y and a quantum system E that is correlated with Y. The von Neumann entropy of the quantum system given Y is denoted as $S(E|Y) = \mathbb{E}_y S(E|Y=y)$. The mutual information between E and Y is $I(E;Y) = S(E) - S(E|Y)$. In CVQKD the following function often occurs in the calculation of entropies,

$$g(x) \stackrel{\text{def}}{=} (x+1)\log_2(x+1) - x\log_2 x. \tag{2}$$

As the figure of merit of a CVQKD scheme we use the Secret Key **Ratio** (or simply key ratio), which equals the length of the constructed secret key divided by the number of laser pulses. This is different from the key *rate* (key bits per second). With the key *ratio* it is possible to do a fair comparison between post-processing schemes of CVQKD setups that have a different number of pulses per second. Note that we do not take into account any pulses that are used solely for channel monitoring.

2.2 CVQKD with Gaussian modulation, homodyne detection and one-way reverse reconciliation

We briefly review the main facts about the secret key capacity in CVQKD. We restrict ourselves to the case of Gaussian modulation, since this will simplify the analysis. We consider the usual attacker model: Eve is allowed to manipulate the quantum states that Alice sends to Bob, but she cannot access or influence their laboratories. In particular, Eve has no influence on Bob's electronic noise ('trusted noise'). We will neglect electronic noise. Alice and Bob can communicate over a classical channel that is noiseless, insecure, and authenticated.

Alice draws random variables $A_1, A_2 \in \mathbb{R}$ from a Gaussian distribution with zero mean and variance σ_X^2. She prepares a coherent state with displacement (A_1, A_2) and sends it to Bob. Bob randomly measures one of the two quadratures. This procedure is repeated n times. Bob's measurement outcomes are denoted as $Y \in \mathbb{R}^n$. Alice's displacement components that match Bob's choice of quadratures are denoted as $X \in \mathbb{R}^n$.

Alice and Bob monitor the noise in the quantum channel. The channel can be entirely characterised by two parameters [12]: the attenuation T and the excess noise parameter ξ. It holds that $y_i = \sqrt{T}x_i + N_{\text{shot}} + N_{\text{exc}}$ where N_{shot} is shot noise, Gaussian with zero mean and variance $\frac{1}{2}$, and N_{exc} is excess noise, Gaussian with zero mean and variance $T\xi/2$. The variance of Y_i is

$$\sigma_Y^2 = T\sigma_X^2 + \frac{1}{2} + \frac{1}{2}T\xi \qquad \sigma_{Y|X}^2 = \frac{1}{2} + \frac{1}{2}T\xi. \tag{3}$$

Bob informs Alice of his quadrature choices. Bob generates a secret key $K \in \mathcal{K}$, which typically is a hash of some U, where U is an error-correction codeword or a discretisation of Y. He computes information reconciliation data P and sends P to Alice. Typically P contains a seed for the hash and e.g. the syndrome of the discretised Y, or a codeword xor'ed into Y. From X and P Alice reconstructs K by first reconstructing U and then hashing U with the provided seed.

The maximum achievable size of K, in bits, divided by n is called the secret key capacity. It has been shown [13] that the secret key capacity for Gaussian modulation and one-way reverse reconciliation is bounded as

$$C_{\text{secr}}^{\text{Gauss}} \geq I(X_i;Y_i) - I(Y_i;E_i). \tag{4}$$

The mutual information between the classical X_i and Y_i follows from the signal-to-noise ratio,

$$I(X_i;Y_i) = \frac{1}{2}\log(1 + \frac{T\sigma_X^2}{\sigma_{Y|X}^2}). \tag{5}$$

In long-distance CVQKD we have $T \ll 1$. In theory it can be advantageous to work with high laser power $\propto \sigma_X^2$, but in practice this causes phase noise [14], which manifests as excess noise. In order to avoid such problems we will only consider the regime where $T\sigma_X^2 \ll 1$ and furthermore $\xi \ll \sigma_X^2$. In this regime, (5) can be approximated as

$$I(X_i;Y_i) = T\sigma_X^2 \log e + \mathcal{O}(T^2). \tag{6}$$

The mutual information $I(Y_i;E_i) = S(E_i) - S(E_i|Y_i)$ follows from the symplectic eigenvalues ν_1, ν_2 of Eve's pre-measurement state ρ^{E_i} and the symplectic eigenvalue ν_3 of the (homodyne) post-measurement state $\rho_{y_i}^{A_i}$ [12].

$$I(Y_i;E_i) = g(\frac{\nu_1 - 1}{2}) + g(\frac{\nu_2 - 1}{2}) - g(\frac{\nu_3 - 1}{2}), \tag{7}$$

with g the thermal entropy function as defined in Section 2.1 and

$$\nu_{1,2}^2 = \frac{\Delta \pm \sqrt{\Delta^2 - 4D}}{2} \tag{8}$$

$$\Delta \stackrel{\text{def}}{=} V^2 + [2\sigma_Y^2]^2 - 2T(V^2 - 1) \tag{9}$$

$$D \stackrel{\text{def}}{=} \Big[V \cdot 2\sigma_Y^2 - T(V^2 - 1)\Big]^2 \tag{10}$$

where $V = 1 + 2\sigma_X^2$, and

$$\nu_3^2 = V\Big[V - \frac{T(V^2 - 1)}{2\sigma_Y^2}\Big]. \tag{11}$$

In the limit $T\sigma_X^2 \ll 1$, $\xi \ll \sigma_X^2$ the mutual information $I(Y_i;E_i)$ behaves as

$$I(Y_i;E_i) = T\sigma_X^2 \cdot \sigma_X^2 \log \frac{1 + \sigma_X^2}{\sigma_X^2} + \mathcal{O}(T^2). \tag{12}$$

The actual key ratio of a CVQKD protocol in practice equals $\frac{\log|\mathcal{K}|}{n}$ multiplied by the success probability of the error correcting code (1 minus the frame rejection rate P_{rej}). The key ratio is limited by the efficiency β of the employed error-correction code ($\beta < 1$) and by the leakage caused by the reconciliation data P,

$$R_{\text{key}} = (1 - P_{\text{rej}})\frac{\beta I(X;Y) - I(U;PE)}{n}. \tag{13}$$

A high key ratio is obtained by using a highly efficient error-correcting code and leakage-free reconciliation data. Good codes for CVQKD achieve $\beta \approx 0.95$ to 0.99. Leakage-free reconciliation data is achieved either by sending a one-time-pad-encrypted syndrome or by the trick described below in Section 2.3.

2.3 Decoupled reconciliation data

Lemma 2.1 (Lemma 1 in [9]). *Let U and P be independent classical random variables. Let E be a quantum system. Then $I(U;PE) \leq I(UP;E)$.*

Corollary 2.2 (Adapted from [9] to the case of reverse reconciliation). *Let X and Y be the measurement result of Alice and Bob respectively. Let E be Eve's quantum system. Let U be a secret chosen by Bob, independent of Y. Let P be public information reconciliation data computed from Y and U, such that Alice is able to reconstruct U from P and X. Let P be statistically independent from U. Then*

$$I(U;PE) \leq I(Y;E). \tag{14}$$

Proof: Lemma 2.1 gives $I(U;PE) \leq I(UP;E)$. Since P is computed from U and Y, it holds that $\mathsf{H}(\overline{UP}) \leq \mathsf{H}(UY)$ and $I(UP;E) \leq I(UY;E)$. Finally, we use that Bob chooses the U independently of Y, which allows us to write $I(UY;E) = I(Y;E)$. □

Substitution of (14) into (13) gives

$$R_{\text{key}}^{(\text{decoupled})} \geq (1 - P_{\text{FE}})\Big\{\beta I(X_i;Y_i) - I(Y_i;E_i)\Big\} \tag{15}$$

which provides a particularly easy way to evaluate the key ratio of a protocol. In [9] the decoupling of C from U is achieved by taking 8-dimensional subspaces and using the algebraic properties of octonions.

2.4 Key establishment from classical noisy channels

Definition 2.3 (Def. 2 in [15]). *Let (X, Y, Z) be jointly distributed classical variables, where Alice holds X, Bob holds Y, and Eve holds Z. Consider a sequence of experiments generating XYZ many times independently. The* **secret key rate** *of X and Y with respect to Z, denoted as $S(X;Y||Z)$, is the maximum rate at which Alice and Bob can agree on a secret key, with public discussion, while keeping the rate at which Eve obtains information about this key arbitrarily small.*

Lemma 2.4 (Theorems 5 and 6 in [15]). *The secret key rate of X and Y with respect to Z is bounded as*

$$S(X;Y||Z) \geq \max\Big[I(Y;X) - I(Z;X),\ I(X;Y) - I(Z;Y)\Big] \tag{16}$$

$$S(X;Y||Z) \leq \min\Big[I(X;Y),\ I(X;Y|Z)\Big]. \tag{17}$$

The capacity lower bound (4) for the case where Z is a quantum system has the same form as (16).

2.5 Useful lemmas

Lemma 2.5. *Let $X_1, \cdots, X_n$ be Gaussian random variables with mean μ_i and unit variance. The distribution of the variable $Z = \sum_{i=1}^{n} X_i^2$ is the noncentral chi-square distribution with n degrees of freedom and noncentrality parameter $\lambda = \sum_{i=1}^{n} \mu_i^2$. The expected value of Z is $n + \lambda$, and the variance is $2n + 4\lambda$. The cumulative distribution of Z is given by $F_Z(z) = 1 - Q_{\frac{n}{2}}(\sqrt{\lambda}, \sqrt{z})$, where Q is the Marcum Q-function.*

Lemma 2.6 (Adapted[1] from Eq.(4.3) in [16]). *Let $\mu \in [0, \infty)$. In the limit of large arguments the Marcum Q-function asymptotically converges to an expansion of the form*

$$Q_\mu(r,s) \sim \frac{1}{2}\mathrm{Erfc}(-\chi) + \frac{\exp(-\chi^2)}{\sqrt{2\pi r s}} \sum_{j=0}^{\infty} c_{2j} \frac{\Gamma(j+\frac{1}{2})}{\Gamma(\frac{1}{2})} (\frac{2}{rs})^j \tag{18}$$

$$\chi = \sqrt{\frac{1}{2}(r^2+s^2) - \sqrt{r^2 s^2 + \mu^2} + \mu(\mathrm{arsinh}\frac{\mu}{rs} - \ln\frac{s}{r})} \tag{19}$$

where the coefficients c_{2j} are complicated functions of μ, r, s.

Lemma 2.7 (Neyman-Pearson). *Let $X \in \mathcal{X}$ be a random variable distributed according to $X \sim P_\theta$, where either $\theta = 0$ or $\theta = 1$. A hypothesis test function is a function $f : \mathcal{X} \to \{0, 1\}$ that tries to determine the parameter θ from the observed data x. Let $\mathbb{E}_{X\sim P_0} f(X)$ be the type I error probability of the test function, and $\mathbb{E}_{X\sim P_1}[1 - f(X)]$ the type II error probability. The likelihood ratio test with threshold k is given by*

$$\varphi_k(x) = \begin{cases} 1: & \frac{P_1(x)}{P_0(x)} > k \\ 0: & \frac{P_1(x)}{P_0(x)} < k \end{cases}. \tag{20}$$

At a fixed type I error probability, the likelihood ratio test (20) has the lowest type II error probability of all test functions.

Lemma 2.8. *A test function obtained by applying a monotone function to the likelihood ratio $\frac{P_1(x)}{P_0(x)}$ and to the threshold is equivalent to the likelihood ratio test.*

3 The proposed information reconciliation method

The random-codebook error correction serves as a first step that produces a low-noise binary string, which can then be further corrected using standard binary codes.

[1] Temme presents the Q-function in a slightly different form, $Q_\mu(\sqrt{2r}, \sqrt{2s})$.

3.1 Protocol steps

Preparation.
Alice and Bob agree on a number of public parameters: a variance σ_X^2; sequence length n; code size q; a random table $w \in [0,1]^{q\times n}$; an integer N; key length L. They agree on a strong extractor function $\mathrm{Ext} : \mathcal{R} \times \{0,1\}^{N\log q} \to \{0,1\}^L$. Furthermore they agree on a binary error-correcting code $\mathcal{E}$ that has codewords of length $N \log q$.
We assume that the channel properties T, ξ are known to Alice and Bob. We write F_Y for the cumulative distribution function of Y, where Y is Gaussian with zero mean and variance σ_Y^2. Alice has a (public) threshold value θ.

Repeated steps (see Fig. 1):

1. Alice sends n coherent states to Bob, using Gaussian modulation. The variance of each quadrature is σ_X^2. Alice stores the displacements.
2. For each coherent state, Bob randomly chooses a quadrature to measure. The result of the homodyne measurement is denoted as $y \in \mathbb{R}^n$. He picks a random row index $u \in \{1,\dots,q\}$. For all $i \in \{1,\dots,n\}$ he computes
$$\tilde{y}_i = F_Y(y_i) \in (0,1) \tag{21}$$
and
$$c_i = \tilde{y}_i + w_{ui} \mod 1. \tag{22}$$
Bob sends to Alice his quadrature choices and the vector $c = (c_1,\dots,c_n)$.
3. Alice constructs a vector $x \in \mathbb{R}^n$ that consists of the transmitted displacements in the direction of Bob's quadrature choices. For each candidate row index $\ell \in \{1,\dots,q\}$ she computes a score $S_\ell(x,w,c)$,
$$S_\ell(x,w,c) = \sum_{i=1}^{n} \left[F_Y^{\mathrm{inv}}(c_i - w_{\ell i} \mod 1) - x_i \sqrt{T} \frac{\sigma_Y^2}{T\sigma_X^2} \right]^2 . \tag{23}$$
If there exists exactly one index ℓ satisfying $S_\ell < \theta$ then Alice sets $\hat{u} = \ell$ and she `accepts`. In any other case she `rejects`. Alice informs Bob of her `accept`/`reject` decision.

Finalization.
Alice and Bob collect the indices $u^{(1)},\dots,u^{(N)}$ from N `accepted` rounds. They convert each of these indices to binary representation and concatenate them; then they use the code $\mathcal{E}$ to get rid of the leftover errors[2] (`accept` events with $\hat{u} \neq u$); finally they do privacy amplification. The final QKD key is
$$\mathrm{Ext}\Big(r, \mathrm{bin}\, u^{(1)} || \dots || \mathrm{bin}\, u^{(N)}\Big) \in \{0,1\}^L. \tag{24}$$
Here r is a randomly chosen (public) seed, and 'bin' stands for binarisation.

3.2 Statistical decoupling

The decoupling between the information reconciliation data (w,c) and the codeword index u, required for the use of Corollary 2.2, is ensured by the uniformity of $\tilde{Y}_i$, combined with the modulo-1 addition. Adding the uniform variable $\tilde{Y}_i$ to w_{ui} modulo 1 is the analog version of a one-time-pad xor mask, and completely hides w_{ui}.

Lemma 3.1. *Let C be constructed as in Section 3.1, $c_i = \tilde{y}_i + w_{ui} \mod 1$. Let $P = (W,C)$. Then the variables P and U are independent.*

Proof: $f_{U|WC}(u|wc) = \frac{f_{UWC}(uwc)}{f_{WC}(wc)} = \frac{f_U(u) f_W(w) f_{C|UW}(c|uw)}{f_W(w)\mathbb{E}_{u'} f_{C|UW}(c|u'w)} = f_U(u) \frac{\prod_i f_{\tilde{Y}}(c_i - w_{ui} \mod 1)}{\mathbb{E}_{u'} \prod_i f_{\tilde{Y}}(c_i - w_{u'i} \mod 1)}$
$= f_U(u) \frac{1}{\mathbb{E}_{u'} 1} = f_U(u)$. Here we have used that $\tilde{Y}_i$ is uniform on $[0,1]$. □
Note that this mechanism for achieving independence between C and U is more versatile than the trick introduced by [9], which acts only on 8 components of Y at a time. Our procedure works with any sequence length n as a whole.

[2] E.g. Bob sends the one-time-padded syndrome of $\mathrm{bin}\, u^{(1)} || \dots || \mathrm{bin}\, u^{(N)}$ to Alice.

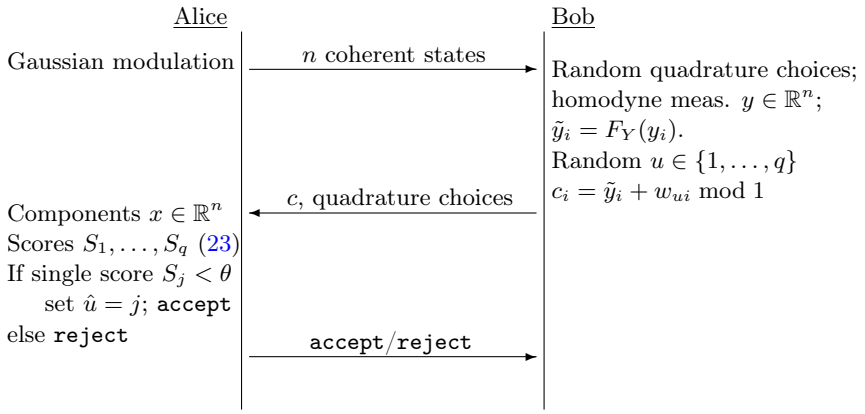

Figure 1: *Protocol steps for information reconciliation of one q-ary symbol u.*

Furthermore, [9] mentions that decoupling cannot be achieved in dimension higher than $d = 8$, because of the requirement that there must exist exactly $d-1$ independent vector fields on the unit sphere in $\mathbb{R}^d$. However, that line of reasoning applies only because they entirely discard the radial degree of freedom in $\mathbb{R}^d$! By *not* discarding the information contained in $|Y|$, we give ourselves the freedom to introduce decoupling as in (22) simply via the uniform $\tilde{y}_i$.

3.3 Motivation of the score function (23)

Alice is faced with a one-out-of-q decision problem. This type of problem does not have a known optimal solution. Instead we resort to an often used alternative: to run q binary decision problems. For each candidate row index $\ell \in \{1, \ldots, q\}$ Alice tests the binary hypothesis "does u equal ℓ?" given the data (x, w, c) available to her. For the *binary* hypothesis test we know that the optimal solution is to use the Neyman-Pearson score (20), i.e. the likelihood ratio, or a monotone function of it. The q individual scores can then somehow be combined to obtain a one-out-of-q decision. One example would be to decide on the index ℓ with the highest Neyman-Pearson score; this is similar to a Maximum A Posteriori (MAP) approach. Instead we work with a threshold that is applied to each individual Neyman-Pearson score. Our motivation for this choice is that it lends itself to analysis.
Below we show that the score (23) is equivalent to the Neyman-Pearson score.

Lemma 3.2. *Consider the hypothesis testing problem of Lemma 2.7. Using the expression* $\Pr[\theta = 1|X = x]$ *as a score function is equivalent to using the likelihood ratio as a score function.*

Proof:

$$\begin{aligned}\frac{P_1(x)}{P_0(x)} &= \frac{\Pr[X = x|\theta = 1]}{\Pr[X = x|\theta = 0]} = \frac{\Pr[X = x]\Pr[\theta = 1|X = x]/\Pr[\theta = 1]}{\Pr[X = x]\Pr[\theta = 0|X = x]/\Pr[\theta = 0]} = \frac{\Pr[\theta = 0]}{\Pr[\theta = 1]} \cdot \frac{\Pr[\theta = 1|X = x]}{\Pr[\theta = 0|X = x]} \\ &= \frac{\Pr[\theta = 0]}{\Pr[\theta = 1]} \cdot \frac{\Pr[\theta = 1|X = x]}{1 - \Pr[\theta = 1|X = x]}. \end{aligned} \tag{25}$$

It follows that $\Pr[\theta = 1|X = x] = \psi(\frac{P_1(x)}{P_0(x)})$, with $\psi(z) = (1 + \frac{1}{z} \cdot \frac{\Pr[\theta=0]}{\Pr[\theta=1]})^{-1}$. We use that ψ is a monotone increasing function and invoke Lemma 2.8. □

Lemma 3.3. $\Pr[U = \ell|xwc] \propto \exp\left[-\frac{T\sigma_X^2}{2\sigma_Y^2\sigma_{Y|X}^2} S_\ell(x, w, c)\right]$, *with S_ℓ as defined in (23).*

Proof:

$$\Pr[U=\ell|xwc] = \frac{\Pr[U=\ell]f_W(w)f_X(x)f_{C|UWX}(c|\ell wx)}{f_W(w)f_X(x)f_{C|WX}(c|wx)} = \frac{1}{q}\cdot\frac{f_{C|UWX}(c|\ell wx)}{f_{C|WX}(c|wx)} \tag{26}$$

$$\propto f_{C|UWX}(c|\ell wx) = \prod_{i=1}^{n} f_{\tilde{Y}|X}(c_i - w_{\ell i} \bmod 1|x_i) \tag{27}$$

$$\overset{(a)}{=} \prod_i \frac{f_{Y|X}(F_Y^{\rm inv}(c_i - w_{\ell i} \bmod 1)\ |x_i)}{f_Y(F_Y^{\rm inv}(c_i - w_{\ell i} \bmod 1))} \tag{28}$$

$$\propto \prod_i \exp -\left(\frac{[F_Y^{\rm inv}(c_i - w_{\ell i} \bmod 1) - x_i\sqrt{T}]^2}{2\sigma^2_{Y|X}} - \frac{[F_Y^{\rm inv}(c_i - w_{\ell i} \bmod 1)]^2}{2\sigma_Y^2}\right) \tag{29}$$

$$\propto \prod_i \exp -\frac{\sigma_Y^2 - \sigma^2_{Y|X}}{2\sigma_Y^2\sigma^2_{Y|X}}\left[F_Y^{\rm inv}(c_i - w_{\ell i} \bmod 1) - x_i\sqrt{T}\frac{\sigma_Y^2}{\sigma_Y^2 - \sigma^2_{Y|X}}\right]^2. \tag{30}$$

In (a) we used that for a monotone function φ the pdf of $Z = \varphi(Y)$ is given by $f_{Z|X}(z|x) = f_{Y|X}(y|x)/\varphi'(y) = \frac{f_{Y|X}(\varphi^{\rm inv}(z)\ |x)}{\varphi'(\varphi^{\rm inv}(z))}$. Then the special choice $\varphi = F_Y$ yields $f_{Z|X}(z|x) = \frac{f_{Y|X}(F_Y^{\rm inv}(z)\ |x)}{f_Y(F_Y^{\rm inv}(z))}$. Finally, the z in this expression equals $\tilde{y}_i$ given $u = \ell$, w and c, which evaluates to $\tilde{y}_i = c_i - w_{\ell i} \bmod 1$. □

Finally, since $\exp[-\text{const}\cdot S_\ell]$ is a monotone function of S_ℓ, our score function (23) is equivalent to the Neyman-Pearson score. Due to the minus sign, a *low* score indicates a high likelihood that that the hypothesis is true.

3.4 Thresholding; error types

Alice's decision procedure leads to a number of cases that can occur, listed in the table below.

Case	Scores	Decision	
1	$S_u < \theta$, $\forall_{\ell\neq u} S_\ell > \theta$	`accept`	True Accept
2	$S_u > \theta$, $\exists_{\text{unique }\ell} S_\ell < \theta$	`accept`	False Accept
3	$S_u > \theta$; $S_\ell < \theta$ for several ℓ	`reject`	justified reject
4	$\forall_\ell S_\ell > \theta$	`reject`	S_u might be smallest score
5	$S_u < \theta$, $\exists_{\ell\neq u} S_\ell < \theta$	`reject`	S_u might be smallest score

An alternative procedure could be to always accept the row index with the lowest score. In cases 4 and 5 that would be likely to extract correct information, whereas our scheme discards the data. However, case 3 would certainly produce a symbol error, and case 4 and 5 would potentially cause a symbol error. Analysis of different decision procedures is left for future work.

4 Analysis

4.1 Statistics of the scores

Lemma 4.1. *Consider the score system for given x, w, u and random Y. The true-codeword score S_u can be written as*

$$S_u(x, w, C) = \sigma^2_{Y|X} A \tag{31}$$

where A follows a noncentral chi-square distribution with parameters (n, λ_1),

$$\lambda_1 = n\frac{\sigma^2_{Y|X}}{T\sigma_X^2}\cdot\frac{\frac{1}{n}\sum_i x_i^2}{\sigma_X^2} \approx n\frac{\sigma^2_{Y|X}}{T\sigma_X^2}. \tag{32}$$

Proof: At $\ell = u$ the expression $F_Y^{\rm inv}(C_i - w_{\ell i} \bmod 1)$ evaluates to $F_Y^{\rm inv}(\tilde{Y}_i) = Y_i$. This yields $S_u(x, w, C) = \sum_i [Y_i - x_i\sqrt{T}\frac{\sigma_Y^2}{T\sigma_X^2}]^2$. We write $Y_i = x_i\sqrt{T} + \sigma_{Y|X}N_i$, where the noise N_i is normal-distributed and independent of all other variables. We get $S_u = \sigma^2_{Y|X}\sum_{i=1}^n [N_i - x_i\sqrt{T}\frac{\sigma_{Y|X}}{T\sigma_X^2}]^2$. This

has the form of $\sigma_{Y|X}^2$ times a noncentral χ^2 variable with n degrees of freedom and noncentrality parameter $\lambda = \sum_i (x_i \sqrt{T} \frac{\sigma_{Y|X}}{T\sigma_X^2})^2$. □

Lemma 4.2. *Consider the score system for given x, y, u and random W. Let the table components $W_{\ell i}$ be independent and uniform on $[0,1]$. Then the wrong-codeword score S_ℓ ($\ell \neq u$) can be written as*

$$S_\ell(x, W, C) = \sigma_Y^2 B_\ell \tag{33}$$

where the random variables $(B_\ell)_{\ell \neq u}$ are independent and follow a noncentral chi-square distribution with parameters (n, λ_0), with

$$\lambda_0 = n \frac{\sigma_Y^2}{T\sigma_X^2} \cdot \frac{\frac{1}{n}\sum_i x_i^2}{\sigma_X^2} \approx n \frac{\sigma_Y^2}{T\sigma_X^2}. \tag{34}$$

Proof: At $\ell \neq u$ the expression $C_i - W_{\ell i} \bmod 1$ evaluates to $\tilde{y}_i + W_{ui} - W_{\ell i} \bmod 1$. Since all the $W_{\ell i}$ are independent and uniform, we find that $F_Y^{\text{inv}}(\tilde{y}_i + W_{ui} - W_{\ell i} \bmod 1)$ is an independent Gaussian variable with zero mean and variance σ_Y^2. Crucially, it is independent of x. We can write $S_\ell = \sum_{i=1}^n [\sigma_Y M_{\ell i} - x_i \sqrt{T} \frac{\sigma_Y^2}{T\sigma_X^2}]^2$, where the $M_{\ell i}$ are independent and normal-distributed. Written as $S_\ell = \sigma_Y^2 \sum_{i=1}^n [M_{\ell i} - x_i \sqrt{T} \frac{\sigma_Y}{T\sigma_X^2}]^2$ we see that each score equals σ_Y^2 times a noncentral chi-squared variable with n degrees of freedom and noncentrality parameter $\lambda = \sum_i (x_i \sqrt{T} \frac{\sigma_Y}{T\sigma_X^2})^2$. □

The two above lemmas will allow us to analytically compute decision error probabilities under the assumption that the codeword table W is completely uniform. For *pseudorandom* W, Lemma 4.1 still holds, but Lemma 4.2 breaks down. Note, however, that for unknown U, Y the argument of $F_Y^{\text{inv}}(\tilde{Y}_i + W_{Ui} - W_{\ell i} \bmod 1)$ is close to uniform when the table size q is large (ergodicity of W). Thus, even though the scores S_ℓ ($\ell \neq u$) are not independent for pseudorandom W, the distribution of each S_ℓ viewed individually will closely resemble the chi-square distribution specified in Lemma 4.2.

4.2 Analytic estimates for the error probabilities

We introduce the following notation for error probabilities,

$$\pi_1 \quad \stackrel{\text{def}}{=} \quad \Pr[S_u > \theta] = Q_{\frac{n}{2}}(\sqrt{\lambda_1}, \sqrt{\frac{\theta}{\sigma_{Y|X}^2}}) \tag{35}$$

$$\pi_0 \quad \stackrel{\text{def}}{=} \quad \Pr_{W \sim \text{unif}}[S_\ell < \theta] = 1 - Q_{\frac{n}{2}}(\sqrt{\lambda_0}, \sqrt{\frac{\theta}{\sigma_Y^2}}) \qquad \ell \neq u. \tag{36}$$

Here Q is the Marcum Q-function as mentioned in Section 2.5. In words, π_1 is the probability that the correct index u gets a score that is on the wrong side of the threshold (high); π_0 is the probability that an incorrect index $\ell \neq u$ gets a score that is on the wrong side of the threshold (low).

Lemma 4.3. *Under the assumption of uniform W, the probability of True Accept (TA) and False Accept (FA) are given by*

$$P_{\text{TA}} = \mathbb{E}_u \Pr[S_u < \theta] \prod_{\ell : \ell \neq u} \Pr[S_\ell > \theta] \tag{37}$$

$$= (1 - \pi_1)(1 - \pi_0)^{q-1} \tag{38}$$

$$P_{\text{FA}} = \mathbb{E}_u \Pr[S_u > \theta] \sum_{a : a \neq u} \Pr[S_a < \theta] \prod_{\ell \notin \{u, a\}} \Pr[S_\ell > \theta] \tag{39}$$

$$= (q-1)\pi_1 \pi_0 (1 - \pi_0)^{q-2}. \tag{40}$$

Proof: (37) and (39) follow from the protocol description in Section 3.1. Lines (38) and (40) follow by substituting (35,36). □

The symbol error rate is defined as the probability of a accepting a row index other than u, conditioned on `accept`.

$$\sigma \stackrel{\text{def}}{=} \Pr[S_u > \theta \wedge \exists_{\text{unique } \ell \neq u} S_\ell < \theta \mid \texttt{accept}] = \frac{P_{\text{FA}}}{P_{\text{TA}} + P_{\text{FA}}}. \tag{41}$$

Corollary 4.4. *Under the assumption of uniform W, the symbol error rare is given by*

$$\sigma = \frac{(q-1)\pi_0\pi_1}{(1-\pi_1)(1-\pi_0) + (q-1)\pi_0\pi_1}. \tag{42}$$

Proof: Follows from substitution of (38,40) into (41). □

From (38) we see that π_0 must not be larger than $\mathcal{O}(\frac{1}{q})$, otherwise the true `accept` probability goes to zero.

4.3 Asymptotics

Upon `accept`, Bob has communicated $\log q$ bits of information to Alice. For some parameter value γ we will enforce the condition

$$\log q = \gamma I(X;Y). \tag{43}$$

Using (5) we can rewrite this condition as

$$\ln q = \gamma \frac{n}{2} \ln(1 + \frac{T\sigma_X^2}{\sigma_{Y|X}^2}) \approx \gamma n \frac{T\sigma_X^2}{2\sigma_{Y|X}^2}, \tag{44}$$

where we used $T\sigma_X^2 \ll 1$. Since there is a clear limit to the value of q that can be implemented in practice, we will treat q as a constant and use (44) to tune σ_X as a function of other system parameters,

$$T\sigma_X^2 \approx \frac{2\sigma_{Y|X}^2 \ln q}{n\gamma}. \tag{45}$$

With (45), we look again at the score statistics. Fig. 2 sketches the pdf of the true-symbol score S_u and the wrong-symbol score S_ℓ ($\ell \neq u$).

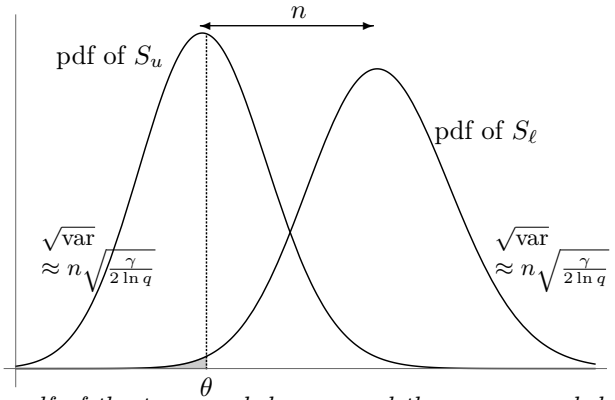

Figure 2: *Sketch of the pdf of the true-symbol score and the wrong-symbol score. The area of the shaded region is π_0. The distance between the pdfs as well as the width of both pdfs are approximately linear in n.*

For the left curve we have (see Lemma 2.5)

$$\lambda_1 \approx n\frac{\sigma_{Y|X}^2}{T\sigma_X^2} \approx \frac{n^2\gamma}{2\ln q} \tag{46}$$

$$\mathbb{E}S_u = \sigma_{Y|X}^2(n+\lambda_1) \approx \frac{n}{2} + \frac{n^2\gamma}{4\ln q} + \mathcal{O}(n^2T\xi) \tag{47}$$

$$\text{Var}(S_u) = \sigma_{Y|X}^4(2n+4\lambda_1) \approx \frac{n}{2} + \frac{n^2\gamma}{2\ln q} + \mathcal{O}(n^2T\xi). \tag{48}$$

For the right curve we have

$$\lambda_0 \approx n\frac{\sigma_Y^2}{T\sigma_X^2} \approx \frac{n^2\gamma}{2\ln q} + n - \mathcal{O}(n^2T\xi) \tag{49}$$

$$\mathbb{E}S_\ell = \sigma_Y^2(n+\lambda_0) \approx \frac{n^2\gamma}{4\ln q} + \frac{3}{2}n + \mathcal{O}(1) - \mathcal{O}(n^2T\xi) \tag{50}$$

$$\mathrm{Var}(S_\ell) = \sigma_Y^4(2n+4\lambda_0) \approx \frac{n^2\gamma}{2\ln q} + \frac{3}{2}n + \mathcal{O}(1) - \mathcal{O}(n^2T\xi). \tag{51}$$

Neglecting $nT\xi \ll 1$, we get the following distance between the pdf centers,

$$\mathbb{E}S_\ell - \mathbb{E}S_u \approx n. \tag{52}$$

We see that our reconciliation system has to deal with the overlap of two pdfs whose centers are separated by a distance n, while both curves have a width that is also of order n, namely $\approx n\sqrt{\frac{\gamma}{2\ln q}}$. This scaling is a consequence of the imposed relation (45) between σ_X, n and q. The only way to reduce the overlap (and thereby improve the reconciliation) is to increase q or to decrease γ.
Since it is of crucial importance to have a low value of π_0, the threshold θ cannot be set far to the right of $\mathbb{E}S_u$. This will inevitably result in a non-negligible π_1, potentially even $\pi_1 \approx \frac{1}{2}$.
According to the Central Limit Theorem, adding a large number of random variables yields a sum that is close to gaussian-distributed. Typically the approximation holds very well near the center of the distribution, but not necessarily in the tails. Hence, estimating π_1 by taking a Gaussian approximation of the S_u score distribution (near $\theta = \mathbb{E}S_u$) is highly accurate, but we have to be careful with the tail of the S_ℓ distribution. The lemma below shows that we are lucky, and that in fact the Gaussian approximation works rather well for the noncentral chi-square distribution.

Lemma 4.5. *Let the threshold be set as $\theta = \mathbb{E}S_u + n\alpha$, with $\alpha < 1$. Let $nT\xi \ll 1$. Then asymptotically for large n it holds that*

$$\pi_0 \sim \frac{1}{2}\mathrm{Erfc}\left([1-\alpha]\sqrt{\frac{\ln q}{\gamma}}\right). \tag{53}$$

Proof: The π_0 is defined according to (36). We use Lemma 2.6 with $\mu = n/2$, $r = \sqrt{\lambda_0} = \sqrt{\frac{n^2\gamma}{2\ln q} + n}$ and $s = \sqrt{\theta/\sigma_Y^2} \approx \sqrt{\frac{n^2\gamma}{2\ln q} + 2\alpha n}$. Note that $r = \mathcal{O}(n)$ and $s = \mathcal{O}(n)$. The expressions contained in the quantity χ (19) are approximated as follows. First, $\sqrt{r^2s^2+\mu^2} = rs\sqrt{1+(\frac{\mu}{rs})^2}$ $= rs[1 + \frac{\mu^2}{2r^2s^2} + \mathcal{O}((\frac{\mu}{rs})^4)]$. This yields $\frac{r^2+s^2}{2} - \sqrt{r^2s^2+\mu^2} = \frac{1}{2}(r-s)^2 - \frac{\mu^2}{2r^2s^2} + \mathcal{O}(\frac{1}{n^2}) = \frac{\ln q}{\gamma}(-\alpha+\alpha^2) + \mathcal{O}(\frac{1}{n})$. Furthermore, $\mu\,\mathrm{arsinh}\frac{\mu}{rs} = \frac{\mu^2}{rs} + \mathcal{O}(\frac{1}{n^2}) = \frac{\ln q}{2\gamma} + \mathcal{O}(\frac{1}{n})$. Finally, $-\mu\ln\frac{s}{r} = \mu\frac{1}{2}\ln\frac{1+\frac{2\ln q}{n\gamma}}{1+2\alpha\frac{2\ln q}{n\gamma}} = \frac{\ln q}{2\gamma}(1-2\alpha) + \mathcal{O}(\frac{1}{n})$. Combining the pieces yields $\chi^2 = \frac{\ln q}{\gamma}(1-\alpha)^2 + \mathcal{O}(\frac{1}{n})$ and hence $\chi = (1-\alpha)\sqrt{\frac{\ln q}{\gamma}} + \mathcal{O}(\frac{1}{n})$. We note that the expression $\exp(-\chi^2)/\sqrt{rs}$ in front of the summation in (18) is of order $\mathcal{O}(\frac{1}{n})$. We mention that $c_0 = \mathcal{O}(1)$. (See [16] for details.) The summation $\sum_j$ is organised such that consecutive terms become smaller and the sum converges to $\mathcal{O}(1)$. Hence the entire contribution containing the $\sum_j$ is of order $\mathcal{O}(\frac{1}{n})$. As a last step we rewrite $1 - \frac{1}{2}\mathrm{Erfc}(-\chi)$ as $\frac{1}{2}\mathrm{Erfc}(\chi)$. □

Corollary 4.6. *Let α and γ be tuned such that $\frac{1-\alpha}{\sqrt{\gamma}} = \frac{1}{\sqrt{\ln q}}\mathrm{Erfc}^{\mathrm{inv}}(2\frac{c}{q-1})$, with $c < 1$ a constant. Then $\pi_0 \approx \frac{c}{q-1}$, and*

$$P_{\mathrm{TA}} \approx e^{-c}(1-\pi_1) \quad ; \quad P_{\mathrm{FA}} \approx ce^{-c}\pi_1 \quad ; \quad P_{\mathrm{ACC}} = e^{-c}[1-(1-c)\pi_1] \tag{54}$$

$$\sigma \approx \frac{c\pi_1}{1-\pi_1+c\pi_1}. \tag{55}$$

Proof: The value of π_0 follows directly by substituting the provided $\frac{1-\alpha}{\sqrt{\gamma}}$ into (53). Next we substitute $\pi_0 \approx \frac{c}{q-1}$ into (38), (40), and (41), using the limit $(1-\frac{c}{q-1})^{q-1} \to e^{-c}$ for $q \gg 1$. □

Example: Choosing e.g. $q = 2^{20}$ and $c = 0.01$ requires $\frac{(1-\alpha)^2}{\gamma} \approx 1.067$, which is not too far away from 1 and can be achieved with a slightly negative α and γ slightly below 1. The combination $q = 2^{20}$, $c = 10^{-3}$ requires $\frac{(1-\alpha)^2}{\gamma} \approx 1.141$.
Note that $\alpha \approx 0$ leads to $\pi_1 \approx \frac{1}{2}$ which implies a true acceptance probability P_{TA} considerably smaller than 1. The symbol error rate, however, is proportional to c and hence it can still be advantageous to choose c small.

4.4 Secret key ratio

4.4.1 Secret key ratio at small T in general

Let us first study the general equation (15) for the key ratio. In the regime $T\sigma_X^2 \ll 1$, $\xi \ll \sigma_X^2$, we can write

$$\beta I(X_i;Y_i) - I(Y_i;E_i) = T\log(e)\cdot\sigma_X^2\left[\beta - \sigma_X^2\ln(1+\frac{1}{\sigma_X^2})\right] + \mathcal{O}(T^2). \tag{56}$$

At given β ($\beta < 1$), the value of σ_X^2 that maximizes $R_{\text{key}}^{(\text{decoupled})}$ scales as $\sigma_X^2 \approx \frac{1}{\sqrt{3}\sqrt{1-\beta}}$. When β is exactly 1, it is in theory advantageous to increase σ_X to infinity. However, the proportionality $1/\sqrt{1-\beta}$ means that the optimal σ_X^2 drops very rapidly; e.g. at $\beta = 0.95$ the optimal σ_X^2 has alreay dropped to $\mathcal{O}(1)$.
Let us define

$$f_\beta(x) = 2x[\beta - x\ln(1+\frac{1}{x})], \tag{57}$$

so that $\beta I(X_i;Y_i) - I(Y_i;E_i) = \frac{1}{2}T\log(e)f_\beta(\sigma_X^2)$. Note that $\lim_{x\to\infty} f_1(x) = 1$. Fig.3 shows, as a function of β, the value of x that maximizes f_β, as well as the achieved maximum function value.

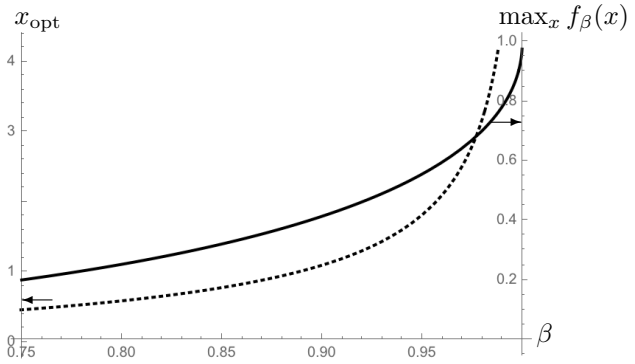

Figure 3: *Solid line:* $\max_x f_\beta(x)$ *as a function of* β. *Dotted line: optimal* x *as a function of* β.

4.4.2 Secret key ratio of our scheme

As mentioned in Section 3.1, the data $u \in \{1,\dots,q\}$ is collected from N runs, and then a binary error correcting code is applied to get rid of residual errors, and finally privacy amplification to get rid of the leakage. We have to take into account that data is added only in case of `accept`; this gives an overall factor of $P_{\text{TA}} + P_{\text{FA}}$, i.e. the accept probability. (This factor also applies to the leakage, since leakage is relevant only with respect to accepted data.) Assuming a good code that performs close to the Shannon limit at low noise level, the error correction leads to a factor $1 - h(\text{BER})$ in the amount of secret data, where BER is the Bit Error Rate. Note that we have to convert the Symbol Error Rate σ (42) to a BER. This is done as follows. Every symbol $\ell \in \{1,\dots,q\}$ has a binary representation. Because of the lack of structure in the table w, a symbol error leads to the acceptance of a *random* row index $\ell \neq u$; hence each bit in the binary representation has a 50%

probability of being flipped. This gives BER $= \sigma/2$. Taking all these considerations into account, we obtain the following key length L,

$$L = (P_{\text{TA}} + P_{\text{FA}}) \cdot N \log q \cdot [1 - h(\frac{\sigma}{2})] - (P_{\text{TA}} + P_{\text{FA}}) Nn \cdot I(E_i; Y_i). \tag{58}$$

The secret key ratio is $R = \frac{L}{Nn}$. With $\log q = \gamma n I(X_i; Y_i)$, we get

$$\begin{aligned} R &= (P_{\text{TA}} + P_{\text{FA}}) \Big[\gamma [1 - h(\frac{\sigma}{2})] I(X_i; Y_i) - I(E_i; Y_i) \Big] & (59) \\ &\overset{(56)}{=} (P_{\text{TA}} + P_{\text{FA}}) T \log(e) \cdot \sigma_X^2 \left[\gamma [1 - h(\frac{\sigma}{2})] - \sigma_X^2 \ln(1 + \frac{1}{\sigma_X^2}) \right] + \mathcal{O}(T^2). & (60) \end{aligned}$$

This expression is of the form (56), with the acceptance probability $P_{\text{TA}} + P_{\text{FA}}$ as a prefactor, and with $\beta = \gamma[1 - h(\frac{\sigma}{2})]$. Note furthermore that the parametrisation (45), $n\sigma_X^2 \approx \frac{\ln q}{T\gamma}$, fixes only the product $n\sigma_X^2$ at given T, q, γ, which seems to imply that we can choose σ_X^2 at will, and n will adapt. However, we cannot indefinitely increase σ_X^2 as that would cause n to decrease to the point where the various terms that we have neglected, such as terms of order $\frac{1}{n}$ and $nT\xi$, become non-negligible.
Note that according to (60), the optimisation of γ, α, σ_X at $T \ll 1$ has practically no dependence on T. This will be apparent in Section 5.

4.4.3 A remark on the secrecy capacity lower bound

Consider a CVQKD scheme that derives the secret key $K \in \{0,1\}^L$ by hashing a discretisation of Y, and where Bob sends a one-time-padded syndrome to Alice . Asymptotically, use of the Leftover Hash Lemma against quantum adversaries yields that the QKD key is secure if $L < S(Y|E)$. If an accept/reject mechanism exists for parts (blocks) of Y, then this condition is modified to $L < P_{\text{ACC}} S(Y|E) = P_{\text{ACC}}[H(Y) - I(E;Y)]$. The achievable secret key ratio is given by $R = (L - \text{syndrome size})/n$, where the size of the syndrome is subtracted because key material is spent to mask the syndrome. The information reconciliation pertains only to the accepted blocks of Y; hence the syndrome size also carries a factor P_{ACC}. Let us write the syndrome size as $P_{\text{ACC}} H(Y|X) \cdot b$. Then[3] the provably safe key ratio is $R < P_{\text{ACC}}[H(Y) - bH(Y|X) - I(E;Y)]/n$ $= P_{\text{ACC}}[\beta I(X;Y) - I(E;Y)]/n$. Hence (15), with the proper relation between β and P_{ACC} inserted, represents a lower bound on the secrecy capacity for any value of β, even $\beta > 1$. Depending on the code, it may happen that (15) achieves a maximum at $\beta > 1$ and that the value exceeds $I(X_i; Y_i) - I(E_i; Y_i)$.

4.4.4 Secrecy capacity upper bound

We conjecture that inequality (17), with the classical Z replaced by Eve's quantum system E, represents an upper bound on the secrecy capacity of CVQKD.

$$\text{Conjecture:} \quad C_{\text{secr}}^{\text{Gauss}} \leq I(X_i; Y_i | E_i). \tag{61}$$

Lemma 4.7. *The conditional mutual information $I(X;Y|E)$ can be written as the Devetak-Winter value plus $S(E|X)$,*

$$I(X;Y|E) = I(X;Y) - I(E;Y) + S(E|X). \tag{62}$$

Proof: We write $I(X;Y|E) = H(Y|E) - H(Y|XE)$ and then repeatedly use the chain rule to re-express entropies conditioned on E as von Neumann entropies of E conditioned on classical variables. Substituting $H(Y|E) = H(Y) + S(E|Y) - S(E)$ and $H(Y|XE) = H(X) + H(Y|X) + S(E|XY) - S(EX) = H(Y|X) + S(E|XY) - S(E|X)$, we get $I(X;Y|E) = H(Y) - H(Y|X) - [S(E) - S(E|Y)] - S(E|XY) + S(E|X) = I(X;Y) - I(E;Y) - S(E|XY) + S(E|X)$. Finally, we note that the post-measurement state ρ_{xy}^E is a pure state, yielding $S(E|XY) = 0$. □
The entropy $S(E|X)$ is computed similarly to $S(E|Y)$.

[3] Typically $b > 1$, meaning that more data is sent than the strictly necessary amount $H(Y|X)$, resulting in $\beta < 1$. A perfect code has $b = 1$ and $\beta = 1$. A code that tries to send a message above the channel capacity has $b < 1$, resulting in $\beta > 1$.

Lemma 4.8.

$$S(E_i|X_i) = g(\frac{\nu-1}{2}), \;\; with \; \nu^2 = 2\sigma_Y^2\Big(1 - T + \frac{T}{1+2\sigma_X^2} + T\xi\Big). \tag{63}$$

Proof: Since E is a purification of the AB system, we can write $S(E_i|X_i) = S(B_i|X_i)$. We derive the covariance matrix B' of the Wigner function for B's post-measurement state after a homodyne measurement on A. (Note that this covariance matrix does not depend on x.) The pre-measurement covariance matrix of AB is

$$\begin{pmatrix} A & C \\ C^T & B \end{pmatrix} = \begin{pmatrix} \mathbf{1}V & \sigma_z\sqrt{T}\sqrt{V^2-1} \\ \sigma_z\sqrt{T}\sqrt{V^2-1} & \mathbf{1}\cdot 2\sigma_Y^2 \end{pmatrix}. \tag{64}$$

We have [12] $B' = B - C^T(XAX)^{\text{inv}}C$, where $X = \left(\begin{smallmatrix}1 & 0\\ 0 & 0\end{smallmatrix}\right)$ and 'inv' stands for the Moore-Penrose inverse. This yields

$$B' = \begin{pmatrix} 2\sigma_Y^2 - \frac{T(V^2-1)}{V} & 0 \\ 0 & 2\sigma_Y^2 \end{pmatrix}. \tag{65}$$

The symplectic eigenvalue ν of B' is given by $\nu^2 = \det B'$. In part of the expression we use $2\sigma_Y^2 = 1 + 2T\sigma_X^2 + T\xi$. □

Corollary 4.9. *It holds that*

$$S(E_i|X_i) = T\frac{\sigma_X^2}{2}\Big(\frac{1}{1+1/2\sigma_X^2} + \frac{\xi}{\sigma_X^2}\Big)\log\Big[\frac{2e}{T\sigma_X^2}\Big(\frac{1}{1+1/2\sigma_X^2} + \frac{\xi}{\sigma_X^2}\Big)^{-1}\Big] + \mathcal{O}(T^2\log\frac{1}{T}). \tag{66}$$

Note that the function $x\ln\frac{e}{x}$ reaches a maximum value 1 at $x = 1$. For $T \ll 1$ it follows that $S(E_i|X_i) \lesssim \log e$, with the maximum achieved at $\sigma_x^2 \approx 2/T$. Note that the information content per photon scales as $S(E_i|X_i)/\sigma_X^2 \propto T$, which is what we are used to see in Discrete-Variable QKD.

5 Numerical results

We present numerical results on the key ratio. At a given T, we parameterize the scheme by setting σ_X^2, q, γ and α. We then set the excess noise to be proportional to the laser power, $\xi = 0.01\cdot\sigma_X^2$. λ_1 and λ_0 follow from (32, 34). The n follows from (43), $n = \frac{\log q}{\gamma I(X_i;Y_i)}$. The threshold θ follows from $\theta = \mathbb{E}S_u + n\alpha = \sigma_{Y|X}^2(n+\lambda_1) + n\alpha$. The error probabilities π_0, π_1 are computed via (35,36). The P_{ACC} and σ follow from Lemma 4.3 and Corollary 4.4. Finally, the secret key ratio is given by (59).[4] We have evaluated the equations numerically using Wolfram Mathematica.
We will denote the Devetak-Winter value (4), which is a function of the channel properties and σ_X^2, by DW. We write maxDW for $\max_{\sigma_X} DW$ at $\xi \to 0$. Without providing details we mention that the numbers shown here are consistent with simulation results.

5.1 Secret key ratio 'landscape'

Fig. 4 shows how the SKR (59) behaves as a function of the parameters α and γ at $T = 0.001$. At smaller T the picture is very similar. There is a long diagonal steep slope in the (α,γ)-plane, to the 'northeast' of the maximum, where the SKR plummets below zero. Note that the SKR is negative at $\gamma < 1$. This is caused by the large modulation variance, which gives rise to a factor $\approx \beta - 1$ in (56). Fig. 5 shows cross sections through the contour plot. Fig. 6 shows dependence on σ_X^2. It is clear that σ_X^2 nontrivially influences the SKR maximisation over α, γ (or vice versa). Fig. 7 shows how the SKR decreases if σ_X^2 and the other scheme parameters are kept constant while the distance increases.

[4] We do not use the large-argument approximations of the Marcum Q function shown in Section 4.3, since it turns out that rather small values of n give good results.

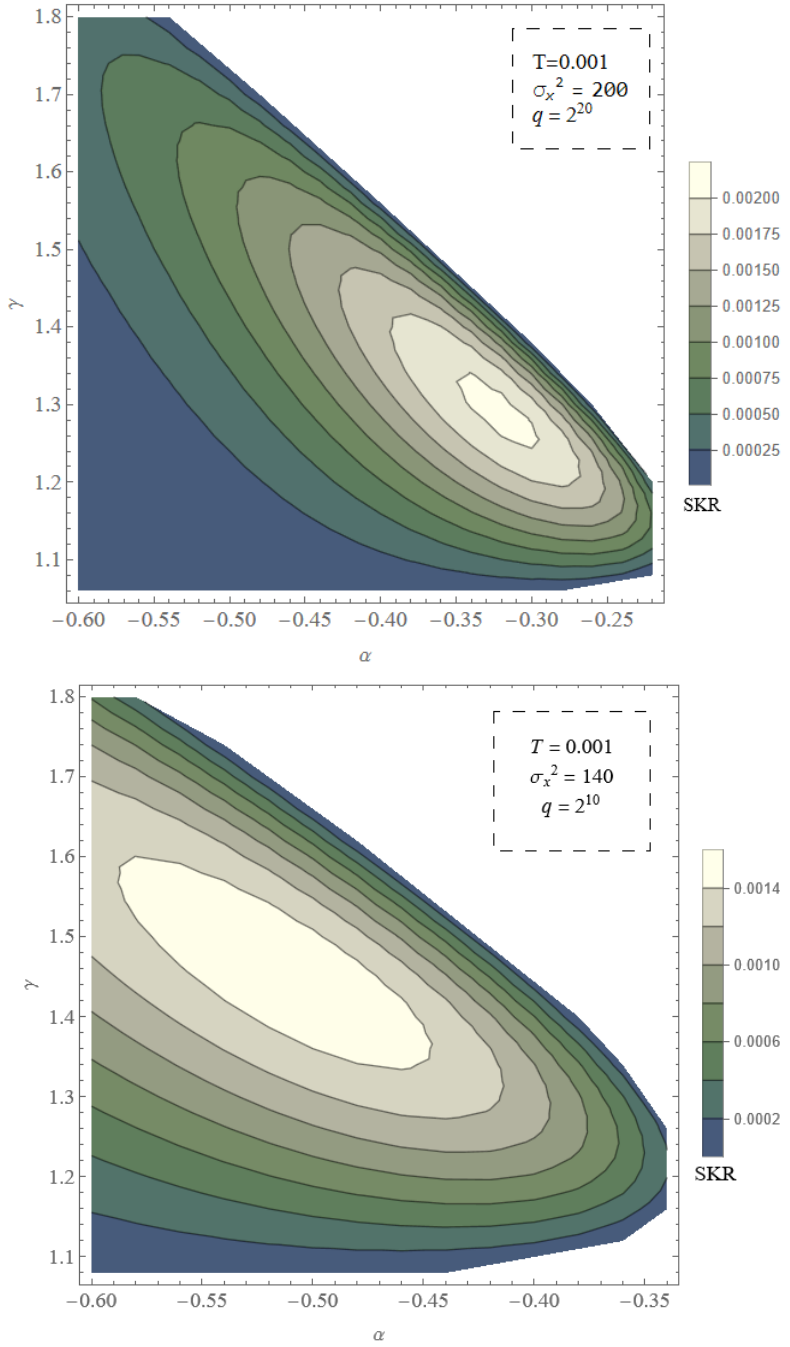

Figure 4: *Contour plots of the Secret Key Ratio as a function of α and γ. Negative SKR is shown as white.*

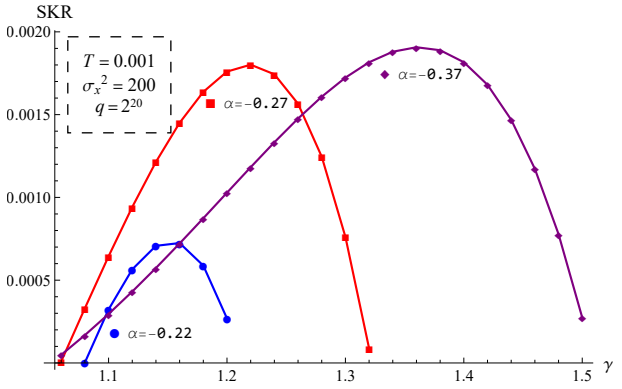

(a) *Secret key ratio as a function of γ for different α.*

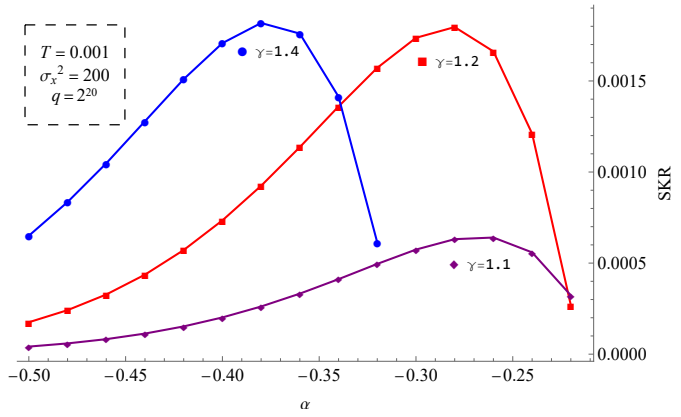

(b) *Secret key ratio as a function of α for different γ.*

Figure 5: *Secret key ratio as a function of α and γ. The T, σ_x^2, q are fixed.*

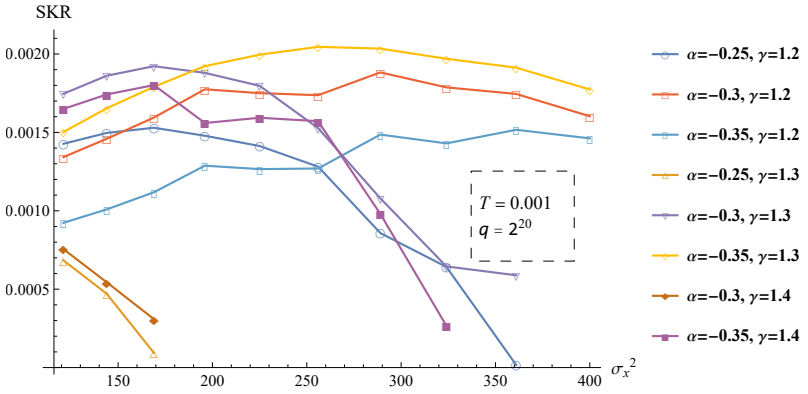

Figure 6: *Secret key ratio as a function of σ_x^2 for different γ and α.*

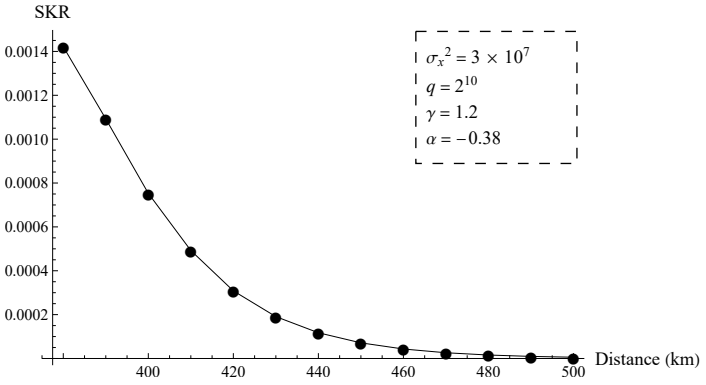

Figure 7: *Secret key ratio as a function of distance for fixed scheme parameters.*

5.2 Optimisation with unrestricted modulation variance

Table 1 shows secret key ratios that we have obtained by tweaking $\alpha, \gamma, \sigma_X^2$ for different values of the transmission T and codebook size q. As observed before, the optimal α and γ do not change much when the distance is increased, but the optimal σ_X^2 scales as $1/T$ as predicted in Section 4.4.4. The obtained SKR values are practically constant as a function of T. This is consistent with the idea of an almost-constant upper bound $I(X_i; Y_i|E_i)$ on the secrecy capacity. Note that our SKR lies far below the asymptote $\log e \approx 1.44$ for the conjectured upper bound.
At $T < 10^{-7}$ it seems that Wolfram Mathematica suffers from numerical instabilities.

Table 1: *Optimised scheme parameters for various values of T and q, without restriction on the modulation variance. The maxDW stands for the maximally achievable Devetak-Winter value at $\xi \to 0$ and depends only on T. The relation between T and distance assumes a loss of 0.22 dB/km.*

T (Distance) MaxDW	q	α	γ	σ_X^2	n	P_{TA}	P_{FA}	SER	SKR
10^{-3} (136 km) 7.2×10^{-4}	2^{10}	-0.51	1.42	163	35	0.047	0.002	0.045	0.0015
	2^{20}	-0.32	1.27	210	55	0.059	0.001	0.020	0.0021
	2^{30}	-0.25	1.23	225	91	0.070	0.0009	0.013	0.0022
10^{-6} (273 km) 7.2×10^{-7}	2^{10}	-0.52	1.42	1.7×10^5	34	0.046	0.002	0.046	0.0015
	2^{20}	-0.33	1.27	2.5×10^5	54	0.057	0.001	0.020	0.0021
	2^{30}	-0.25	1.23	2.2×10^5	92	0.070	0.0009	0.013	0.0022

6 Implementability

The main implementation hurdle is the sheer size of the codebook w: it has $q \times n$ entries, where q is exponential in the message size. One could consider storing the whole codebook in a memory. The drawback is (a) huge memory requirements; (b) long access times fetching table entries. A more practical approach is to pseudorandomly generate codebook entries on the fly without accessing RAM. PRNG algorithms have been reported that generate 64 to 128 bits of pseudorandomness per nanosecond per core [17, 18]. Let b denote the baud rate, i.e. the numer of pulses per second. In the time $1/b$ between pulses, a whole q-element column of the codebook needs to be generated. Hence the required PRNG speed is $q \cdot b$ codebook entries per second, where each entry consists of multiple bits depending on the fine-grainedness of the implementation. Taking for example $q = 2^{10}$, $b = 2^{22}$ results in 2^{32} required entries per second, versus the $\approx 2^{37}$ bits per second that one core can generate. For higher baud rates and larger q many parallel PRNGs will be needed, e.g. implemented on FPGAs.

Note that the quality of the pseudorandom bits may not need to be high. Good error-correcting properties are perhaps achievable with PRNGs that do not pass randomness test suites, and which produce far more bits per clock cycle.
Another computational bottleneck is that Alice needs to evaluate the function F_Y^{inv} for every single codebook entry. Fortunately, all sub-scores can be computed in parallel. The process can be speeded up by first determining all the possible discrete values of $c_i - w_{\ell i}$ and then storing all the possible values of $F_Y^{\text{inv}}(c_i - w_{\ell i} \mod 1)$ in a lookup table (LUT). The squaring operation can similarly be precomputed. This would result in a two-dimensional LUT of sub-score values indexed by discrete values for x_i and $c_i - w_{\ell i} \mod 1$. Computing the score S_ℓ then reduces to counting how often each entry in the LUT occurs in the $\sum_{i=1}^{n}$ summation. It may be possible to store the whole LUT in cache, which can be accessed much faster than general RAM. Similarly, the scores $S_1, \ldots, S_q$ can be kept in cache while 'under construction'.

7 Discussion

The idea of random codebooks is very simple but completely impractical under normal circumstances. In long-distance CVQKD, however, it becomes feasible to consider implementing random codebooks, because of the extremely low code rates. We have investigated this idea, making two design choices: (i) analog xor-ing of Y and a random codeword on the interval $[0, 1]$; (ii) working with a threshold and accepting only if there is a single candidate condeword at the correct side of the threshold. The scoring system is somewhat nontrivial but does not count as a design choice since it follows from standard hypothesis testing.
The analog `xor` on $[0, 1]$ achieves statistical decoupling of C and U in a particularly simple way, without needing 8-component parts of Y. The choice to work with a score threshold was motivated mostly by the wish to define a scheme that can easily be analysed. It has the advantage that it creates a straightforward option for rejecting blocks, hence allowing for trying $\beta > 1$. An alternative method would be to reject if there are no candidate symbols below the threshold, and otherwise accept the symbol with the lowest score.
The numerical analysis shows that secret key ratios can be obtained above the Devetak-Winter value, provided that the modulation variance can be set higher than in current CVQKD setups. For very low T the predicted optimal ratio is orders of magnitude above Devetak-Winter, but it also requires much larger modulation variance $\sigma_X^2 \propto 1/T$. Technical obstacles could occur at such large modulation variance. We note that the optimal key ratio is essentially constant as a function of T, which is consistent with the conjectured upper bound (66). The amount of QKD key material per photon scales as T, which is what happens in Discrete-Variable QKD.
We mention a number of topics for future work.

- Discretisation. The numerics presented in Section 5 assume a very fine-grained discretisation of the interval $[0, 1]$, essentially a continuum. For actual implementation it needs to be determined how coarse the discretisation can be made while still keeping good error-correction performance.
- A more extensive secret key rate analysis, taking into account electronic noise, quantum efficiency and finite size (non-asymptotic) effects.
- Optimized software and hardware implementation, with good parameter choices, pseudorandom generators etc and a binary code for the final error correction step.
- Pseudorandomness. The statistical analysis in Section 4 assumes fully random and independent codebook entries. Simulations should show how much of the analysis stays valid in the case of pseudorandomness, as a function of the seed size and the 'quality' of the PRNG.
- Alternative scoring and decision procedures.
- The (im)practicality of increased modulation variance.

Acknowledgements

We gratefully acknowledge discussions with João dos Reis Frazão, Kadir Gümüş, and Basheer Joudeh. Part of this work was supported by Groeifonds QDNL KAT-2 and by the Forwardt project (NWO CS.001).

References

[1] S.J. Johnson, V.A. Chandrasetty, and A.M. Lance. Repeat-Accumulate codes for reconciliation in Continuous Variable Quantum Key Distribution. In *2016 Australian Communications Theory Workshop (AusCTW)*, pages 18–23.

[2] M. Milicevic, C. Feng, L.M. Zhang, and P.G. Gulak. Key reconciliation with Low-Density Parity-Check codes for long-distance quantum cryptography. 2017. https://arxiv.org/pdf/1702.07740.pdf.

[3] X. Jiang, S. Yang, P. Huang, and G Zeng. High speed reconciliation for CVQKD based on spatially coupled LDPC codes. *IEEE Photon. J.*, 10:1–10, 2018.

[4] D. Guo, C. He, T. Guo, Z. Xue, Q. Feng, and J. Mu. Comprehensive high-speed reconciliation for continuous-variable quantum key distribution. *Quantum Information Processing*, 19, 2020. Article number 320.

[5] K. Gümüş, T.A. Eriksson, M. Takeoka, M. Fujiwara, M. Sasaki, L. Schmalen, and A. Alvarado. A novel error correction protocol for continuous variable quantum key distribution. *Scientific Reports*, 11, 2021. article number 10465.

[6] P. Jouguet and S. Kunz-Jacques. High performance error correction for quantum key distribution using polar codes. *Quantum Information & Computation*, 14(3-4):329–338, 2014.

[7] M. Zhang, H. Hai, Y. Feng, and X.-Q. Jiang. Rate-adaptive reconciliation with polar coding for continuous-variable quantum key distribution. *Quantum Information Processing*, 20, 2021. Article number 318.

[8] S. Yang, Z. Yan, H. Yang, Q. Lu, Z. Lu, L. Cheng, X. Miao, and Y. Li. Information reconciliation of continuous-variables quantum key distribution: principles, implementations and applications. *EPJ Quantum Technology*, 10, 2023. article number 40.

[9] A. Leverrier, R. Alléaume, J. Boutros, G. Zémor, and P. Grangier. Multidimensional reconciliation for a continuous-variable quantum key distribution. *Phys.Rev.A*, 77:042325, 2008.

[10] G. Van Assche, J. Cardinal, and N.J. Cerf. Reconciliation of a quantum-distributed Gaussian key. *IEEE Transactions on Information Theory*, 50(2):394–400, 2004.

[11] S.J Johnson, A.M Lance, L. Ong, M. Shirvanimoghaddam, T.C. Ralph, and T. Symul. On the problem of non-zero word error rates for fixed-rate error correction codes in continuous variable quantum key distribution. *New J. of Physics*, 19:023003, 2017.

[12] Anthony Leverrier. *Theoretical study of continuous-variable quantum key distribution.* Phd thesis, Télécom ParisTech, November 2009.

[13] I. Devetak and A. Winter. Distillation of secret key and entanglement from quantum states. *Proc.R.Soc.A*, 461:207–235, 2005.

[14] A. Marie and R. Alléaume. Self-coherent phase reference sharing for continuous-variable quantum key distribution. *Phys.Rev.A*, 95:012316, 2017.

[15] Ü. Maurer. Secret key agreement by public discussion from common information. *IEE Trans. on Information Theory*, pages 733–742, 1993.

[16] N.M. Temme. Asymptotic and numerical aspects of the noncentral chi-square distribution. *Computers Math. Applic.*, 25(5):55–63, 1993.

[17] S. Vigna. Further scramblings of Marsaglia's xorshift generators. *Journal of Computational and Applied Mathematics*, 315:175–181, 2017.

[18] MWC256 algorithm. https://prng.di.unimi.it/.